The Astrophysical Journal, 728:20 (8pp), 2011 February 10 doi:10.1088/0004-637X/728/1/20

PLANETESIMAL FORMATION BY SUBLIMATION

Etsuko Saito and Sin-iti Sirono
Earth and Environmental Sciences, Nagoya University, Tikusa-ku, Furo-cho, Nagoya 464-8601, Japan
Received 2010 June 22; accepted 2010 November 29; published 2011 January 14

ABSTRACT

This paper proposes a scenario for the formation of rocky plantesimals. In this scenario, the infall of an icy dust aggregate to the central star occurs because of gas drag in the protoplanetary nebula. The temperature of the aggregate rises and H_2O ice sublimates within the snow line. The silicate cores in a dust grain are ejected, following which sublimation occurs. Because the infall velocity of a silicate grain is much less than that of the original aggregate, the silicate cores stagnate in the sublimation region. We calculate the evolution of the dust surface density distribution of the silicate cores. It is shown that the surface density is increased by a factor of 10 or more, which is sufficient to trigger gravitational instability in ∼600 yr after the formation of ∼10 cm sized aggregates.

Key words: methods: numerical – planets and satellites: formation – protoplanetary disks

Online-only material: color figure

1. INTRODUCTION

Although a planetesimal is a key element in planetary formation, its formation process remains controversial. Classically, gravitational instability (Goldreich & Ward 1973) is thought to occur in a laminar gaseous protoplanetary nebula. However, Weidenschilling (1977) pointed out that this instability is inhibited by turbulence that is induced by the velocity difference between the gas and the dust layers. In addition, Sekiya (1998) showed that a dust-to-gas surface density ratio that is 5–20 times greater than normal cosmic values is required. Collisional sticking is thus proposed as an alternative scenario. However, this hypothesis has also been criticized because the maximum collisional velocity between dust aggregates is $\sim 50\,\mathrm{m\,s^{-1}}$, where a collisional outcome is probably a catastrophic disruption.

Many models in which this ratio would be sufficiently increased such that it could trigger gravitational instability have been proposed thus far; these include dust concentration by turbulence eddies (Cuzzi et al. 2001), radial drift of dust aggregates (Youdin & Shu 2002), anticyclonic vortices (Chavanis 2000), streaming instability(Johansen et al. 2007), and photoevaporation by UV rays (Throop & Bally 2005).

These models are applicable for the formation of icy planetesimals. Rocky planetesimals, however, are difficult to explain because the binding energy between silicate materials is extremely low compared to that for icy materials, and rocky dust aggregates are easily broken (Wada et al. 2009). In this study, we propose a robust mechanism for the formation of a rocky planetesimal around the snow line of a protoplanetary nebula. This mechanism is based on the sublimation of the icy mantle that covers a silicate core in a dust grain. The infall of an icy dust aggregate composed of icy dust grains to the central star occurs because of gas drag. The aggregate passing the snow line sublimates the H_2O ice and leaves a silicate core. The silicate core stagnates where it is ejected because its infall velocity is much less than that of the original aggregate. A continuous supply of icy aggregates increases the dust surface density around the snow line, eventually leading to gravitational instability.

Sublimation of ice at the snow line followed by the infalling of icy aggregates has been studied (Stepinski & Valageas 1997; Cuzzi & Zahnle 2004; Ciesla & Cuzzi 2006) because it leads to accumulation of icy particles slightly beyond the snow line. The sublimated H_2O vapor diffuses outward and condenses to form the icy particles and accumulates just outside the snow line. This accumulation may help the formation of planetesimals or Jovian planets. However, there has been less attention on the silicate cores left behind the sublimation.

This paper is organized as follows. The outline of this model is described in the next section. Basic equations regarding the sublimation and infall of an icy dust aggregate are explained in Section 3. In Section 4, the conditions of the numerical simulations are presented, and in Section 5, the results of these numerical simulation are presented. In Section 6, we discuss possible effects that are not included in the simulation. Our conclusions are presented in Section 7.

2. OUTLINE OF MODEL

A micron-sized dust grain consists of a silicate core with an icy mantle. The main component of the ice is H_2O ice. The micron-sized dust grains collide and stick to one another, growing into a dust aggregate (Figure 1). This aggregate can safely grow to a size of up to ∼cm depending on the sticking velocity of an icy particle and their mutual collisional velocity. An icy dust aggregate infalls to the central star because of the gas drag force.

The radial infall velocity of the icy dust aggregate increases with the size of the aggregate. As the icy dust aggregate approaches the central star, its temperature increases. The H_2O ice of the aggregate sublimates as vapor because of the low vapor pressure in a protoplanetary disk.

The H_2O ice of the aggregate sublimates from the surface of the aggregate. When the icy mantle on a grain is completely sublimated, the silicate core of the grain is ejected. Because the silicate core is much smaller (∼micron size) than the icy dust aggregate (typically 10 cm), the radial infall velocity of the silicate core is negligible as compared to that of the original aggregate. The infall of the silicate cores effectively stops and the cores stagnate in the sublimation region. The continuous infall of icy dust aggregates leads to an accumulation of silicate cores in the sublimation region. As a result, the surface density of the silicate cores is increased.

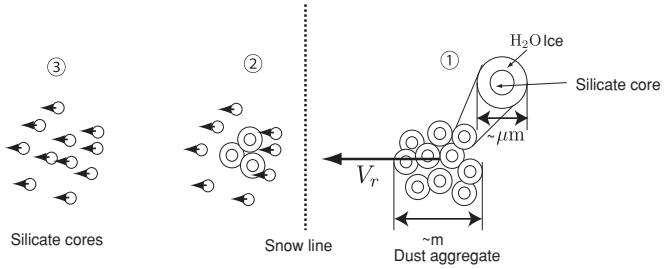

Figure 1. Schematic of this model. An icy dust aggregate consists of icy dust grains, each of which has a silicate core and an icy mantle whose main component is H_2O ice. When the aggregate passes the snow line, the H_2O ice sublimates and silicate cores are ejected from the aggregate. The silicate cores then stagnate because their infall velocity is much less than that of the original aggregate.

3. BASIC EQUATIONS

We assume that an icy dust aggregate is a homogeneous sphere of radius R. The density $\rho_{\rm mat}$ of an icy dust aggregate is given by

$$\rho_{\rm mat} = \phi \left(\rho_{\rm H_2O} + \rho_{\rm sil} \frac{f}{1-f} \frac{\rho_{\rm sil}}{\rho_{\rm H_2O}} \right) \left(\frac{f}{1-f} \frac{\rho_{\rm sil}}{\rho_{\rm H_2O}} + 1 \right)^{-1}, \tag{1}$$

where f is the mass fraction of the silicate cores in an icy dust aggregate, $\rho_{\rm sil}$ is the density of a silicate core, $\rho_{\rm H_2O}$ is the density of H_2O ice, and ϕ is the packing fraction of an icy dust aggregate.

The silicate cores are ejected, followed by sublimation of the H_2O ice. The icy dust aggregate shrinks at the sublimation rate of H_2O ice if we assume the sublimation proceeds only on the surface of the aggregate. The shrinkage rate of the icy dust aggregate is

$$\frac{d}{dt} \left(\frac{4}{3} \pi R^3 \right) = -4\pi R^2 N v_{\rm H_2O}, \tag{2}$$

where $v_{\rm H_2O}$ is the volume of an H_2O molecule, and N is the number of sublimating H_2O molecules per unit surface area and per unit time given by

$$N = \frac{P_{\rm ev}(T) - P_{\rm H_2O}}{\sqrt{2\pi m_{\rm H_2O} k_{\rm B} T}}, \tag{3}$$

where $P_{\rm ev}$ is the equilibrium vapor pressure of H_2O ice, $P_{\rm H_2O}$ is the partial H_2O pressure in the protoplanetary disk, $k_{\rm B}$ is the Boltzmann constant, T is the temperature of the icy dust aggregate, and $m_{\rm H_2O}$ is the mass of an H_2O molecule. We assume temperature $T(r)$, gas surface density $\Sigma_{\rm gas}(r)$, and initial dust surface density $\Sigma_{\rm dust0}(r)$ distributions of (Hayashi et al. 1985)

$$T(r) = 2.8 \times 10^2 \left(\frac{r}{1\,{\rm AU}} \right)^{-1/2} {\rm K} \tag{4}$$

$$\Sigma_{\rm gas}(r) = 1.7 \times 10^3 \left(\frac{r}{1\,{\rm AU}} \right)^{-1/2} {\rm g\,cm^{-3}} \tag{5}$$

$$\Sigma_{\rm dust0}(r) = 4.2 \times 10^1 \left(\frac{r}{1\,{\rm AU}} \right)^{-1/2} {\rm g\,cm^{-3}}. \tag{6}$$

The equilibrium H_2O vapor pressure as a function of T is adopted from Yamamoto et al. (1983) as (in the unit of dyne $\rm cm^{-2}$)

$$\log_{10} P(T)_{\rm ev} = -2445.5646/T + 8.2312 \log_{10} T - 0.01677006T + 1.20514\ 10^{-5} T^2 - 3.63227.$$

Differentiating Equation (2) with respect to time t, and substituting Equation (3), we obtain

$$\frac{dR}{dt} = -\frac{P_{\rm ev}(T) - P_{\rm H_2O}}{\rho_{\rm H_2O}} \sqrt{\frac{m_{\rm H_2O}}{2\pi k_{\rm B} T}}. \tag{7}$$

The radial infall velocity of an icy dust aggregate of radius R is given by (Nakagawa et al. 1986)

$$\frac{dr}{dt} = -\frac{2\Gamma(R)\eta v_{\rm K}}{1+\Gamma(R)^2} \equiv V_r, \tag{8}$$

where $v_{\rm K}$ is the Keplerian velocity, $\eta = -1/2(c_{\rm s}/v_{\rm K})^2 (\partial \ln P/\partial \ln r)$, $c_{\rm s}$ is the sound velocity, and P is the mean gas pressure in a protoplanetary disk given by $P(r) = \Sigma_{\rm gas}(r) k_{\rm B} T / m_{\rm mean} h_{\rm gas}$, where $h_{\rm gas}$ is the gas scale height. $m_{\rm mean}$ is the mean molecular mass of the gas. Γ is the ratio of the Keplerian time to the relaxation time of the gas drag. The approximate formulae for Γ are given by

$$\Gamma = \frac{\Sigma_{\rm gas}}{\rho_{\rm mat} R} \quad \left(R < \frac{3}{2} l_{\rm gas} \right) \tag{9}$$

$$\Gamma = \frac{\Sigma_{\rm gas}}{\rho_{\rm mat} R} \frac{3 l_{\rm gas}}{2R}, \quad \left(R \geqslant \frac{3}{2} l_{\rm gas} \right), \tag{10}$$

where $l_{\rm gas}$ is the mean free path of a gas molecule. According to Equation (8), the radial infall velocity V_r reaches a maximum when $\Gamma = 1$.

Solving Equations (7) and (8) simultaneously, we obtain the relationship between the distance r from the central star and the mass $M(r)$ of the sublimating icy dust aggregate. From this relationship, we can obtain the dust surface density of the ejected silicate cores as

$$\Sigma_{\rm dust}(r) = \frac{1}{2\pi r} \sum_i^N \left(-f \frac{dM_i(r_i)}{dr} \right), \tag{11}$$

where M_i and r_i are the mass and position of the ith aggregate (i runs for *all* aggregates in the nebula), respectively. Note that this surface density only includes that of ejected silicate cores; the contribution from the infalling icy dust aggregates is not included.

The ejected silicate cores collide with the infalling icy dust aggregate. The silicate cores may or may not stick to the aggregate. Here, we estimate the thickness of the silicate core layer that covers the infalling icy dust aggregate.

We assume that the silicate cores are suspended with a surface density distribution of $\Sigma_{\rm dust}(r)$ within a region between $r_{\rm sn0} \leqslant r \leqslant r_{\rm sn}$, and we also assume that the silicate cores stick perfectly to the infalling icy aggregate. If the aggregate does not sublimate the H_2O ice in this region, the thickness ΔR of the silicate core layer on the icy dust aggregate is given by

$$\Delta R = \frac{1}{4\pi\rho_{\rm mat}} \int_{r_{\rm sn0}}^{r_{\rm sn}} \rho_{\rm dust}(r) dr = \frac{1}{4\pi\rho_{\rm mat}} \int_{r_{\rm sn0}}^{r_{\rm sn}} \frac{\Sigma_{\rm dust}(r)}{h_{\rm dust}(r)} dr, \tag{12}$$

where $h_{\rm dust}(r)$ is the scale height of the ejected silicate cores.

4. NUMERICAL SETTINGS

Because a simulation of the evolution of all aggregates in a protoplanetary nebula is untraceable, Equation (11) is simplified as

$$\Sigma_{\rm dust}(r) = \frac{1}{2\pi r}\sum_k \left(-fN_k\frac{dM_k(r_k)}{dr}\right), \qquad (13)$$

where M_k is the mass of the representative aggregate located at r_k. N_k is the number of the representative aggregate. At $t = 0$, $r_k(t = 0)$ is given by $r_k(t = 0) = k\Delta r + r_0$ and N_k is given by $N_k = \Sigma_{\rm dust0}(r_k)\Delta r/M_k$. $\Delta r = 10^{-4}$ AU is adopted. The initial radius R_0 of the aggregates is uniform in the nebula.

The densities of H_2O ice and a silicate core are given by $\rho_{H_2O} = 1.0\,{\rm g\,cm^{-3}}$ and $\rho_{\rm sil} = 2.8\,{\rm g\,cm^{-3}}$, respectively. The packing fraction of an aggregate is $\phi = 0.5$. The mass fraction of silicate core is $f = 0.25$ (Greenberg 1998).

We determine the dust surface density distributions for the following three cases; $P_{H_2O} = 0$, $P_{H_2O} \neq 0$, and $P_{H_2O} \neq 0$, with the sweeping by an infalling aggregate according to Equation (12).

4.1. $P_{H_2O} = 0$

First, we set $P_{H_2O} = 0$ in Equation (7), and we determine the resultant dust surface density distribution. Although neglecting the H_2O vapor pressure is not physically reasonable, the basic features throughout this model are well described by this simulation. The result of this case has common characteristics in the following more realistic cases. The aggregates are initially located between 5 and 45 AU in this model, and we varied the initial aggregate radius, R_0.

4.2. $P_{H_2O} \neq 0$

In this case, the sublimation of an icy aggregate does not proceed beyond the snow line. The H_2O ice sublimes only within the snow line. The sublimation is limited to an extent determined by the equilibrium H_2O vapor pressure. An icy dust aggregate begins to sublimate when it crosses the snow line. The H_2O vapor pressure increases because of sublimation within the snow line. When the H_2O vapor pressure reaches the equilibrium vapor pressure, the sublimation stops and the snow line shifts inward.

The location of the snow line is defined as the distance at which H_2O vapor pressure is equal to the equilibrium H_2O vapor pressure. The initial H_2O vapor pressure distribution can be obtained from the dust surface density distribution (Equation (6)). The H_2O vapor pressure is given by

$$P_{H_2O} = \frac{\Sigma_{H_2O}k_{\rm B}T}{m_{H_2O}h_{\rm gas}}, \qquad (14)$$

where Σ_{H_2O} is the surface density of H_2O vapor which is the sum of the initially distributed H_2O vapor (obtained from Equation (6)) and the fraction $1 - f$ of the sublimated aggregate mass. It should be noted that the scale height of H_2O vapor is the same as that of the main component of the gas. This assumption corresponds to the rapid vertical diffusion of H_2O vapor.

The initial aggregate radius is $R_0 = 10$ cm in this simulation, which is the typical size of the infalling aggregate, as determined by a coagulation equation (Brauer et al. 2008). The result does not depend on the size, as shown later. We determined the evolution of Σ_{H_2O} in addition to $\Sigma_{\rm dust}$. The aggregates are initially distributed between 3 and 75 AU in this simulation.

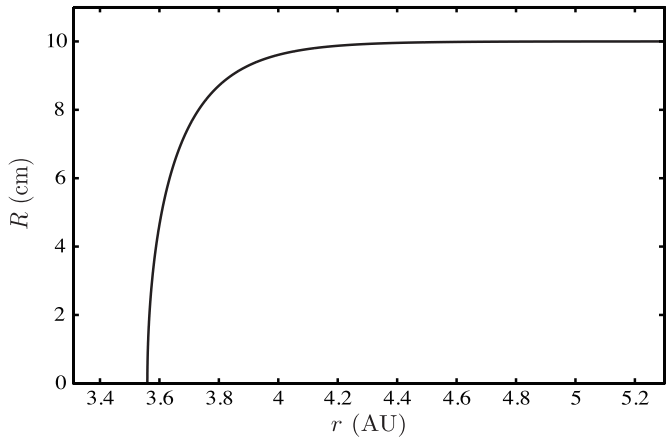

Figure 2. Evolution of the radius R of an icy dust aggregate by infall and sublimation. The initial radius of the icy dust aggregate is 10 cm.

4.3. Sweeping

As an icy dust aggregate passes a region where silicate cores are suspended, it sticks to the silicate cores and grows (Equation (12)) in this region. If an icy dust aggregate covered with silicate cores reaches the snow line, the aggregate sublimates and re-ejects the silicate cores, including those that were sticking to it. As a result, the dust surface density increases more rapidly than in the case without sticking. It is assumed that the swept silicate cores are ejected at the sublimation rate of H_2O ice, as in the previous cases. This assumption will be discussed in Section 6.

We assume that the silicate cores are distributed between the initial snow line $r_{\rm sn0}$ and the shifted snow line $r_{\rm sn}$. We define $\delta = r_{\rm sn0} - r_{\rm sn}$ as the distance between the initial snow line and the shifted snow line. We studied seven cases: $\delta = 0.1$, 0.2, 0.3, 0.4, 0.5, 0.6, and 0.7 AU. The initial radius of an icy dust aggregate is 10 cm. The surface density distribution of the silicate core is given by the simulations described in Section 4.2.

When an icy dust aggregate of radius R_0 passes this region, it sticks to the silicate cores and its radius increases. We can determine this increase in radius ΔR from Equation (12), where $h_{\rm dust}(r)$ is the dust scale height, which is assumed to be $h_{\rm gas}(r)/100$ (N. Ishitsu 2009, private communication). We then carry out the numerical simulations described in the previous subsection. The initial radius of an aggregate is $R = R_0 + \Delta R$ and sublimation begins at the shifted snow line $r_{\rm sn}$. The material density of the outer layer of ΔR is $\phi\rho_{\rm sil}$ when calculating dM/dt in Equation (11).

5. RESULTS

5.1. $P_{H_2O} = 0$

First, we show the results for the case of $P_{H_2O} = 0$. Figure 2 shows the evolution of the radius R of an icy dust aggregate as a function of its position r. The initial radius R_0 of the aggregate is 10 cm. The icy dust aggregate begins to sublimate at 4.4 AU and disappears at 3.6 AU.

As the infall of the aggregate to the central star occurs, the temperature of the aggregate rises. The sublimation rate N (Equation (3)) increases sharply because the equilibrium vapor pressure $P_{\rm ev}(T)$ is exponentially dependent on the temperature. On the other hand, the infall velocity decreases as sublimation proceeds because of the shrinkage of the aggregate (see Equations (7) and (8)). As a result, the radius rapidly decreases to zero with no substantial infall at 3.6 AU.

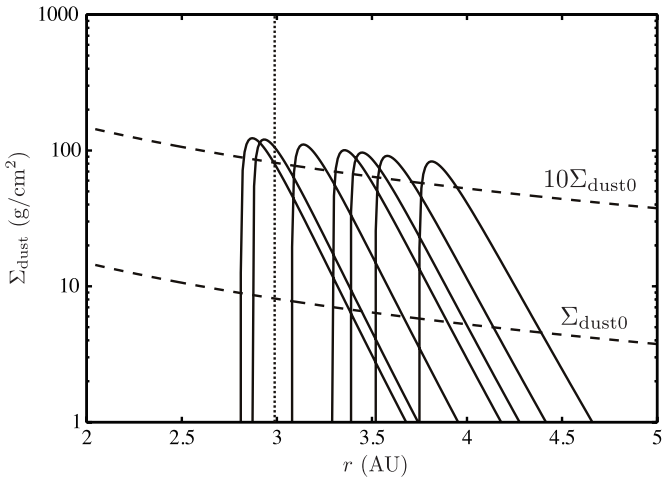

Figure 3. Dust surface density distributions as functions of r for the case of $P_{\rm H_2O} = 0$. From right to left, the initial radius R_0 of the aggregate is 5, 10, 15, 20, 40, 80, and 100 cm. The curve $\Sigma_{\rm dust0}$ is the initial dust surface density distribution given by Equation (6), and $10\Sigma_{\rm dust0}$ is an approximate criterion of the gravitational instability given by 10 times the initial dust surface density. The vertical dotted line at 3.0 AU is the snow line. Note that the peaks for $R_0 < 40$ cm lie beyond the snow line.

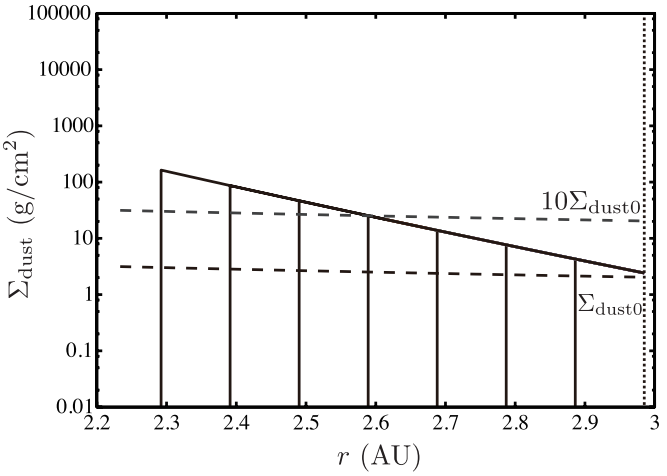

Figure 4. Dust surface density distributions as a function of r for $P_{\rm H_2O} \neq 0$ case. From right to left, distributions for $\delta = 0.1$ AU (6.2×10^2 yr), 0.2 AU (1.6×10^3 yr), 0.3 AU (3.0×10^3 yr), 0.4 AU (4.8×10^3 yr), 0.5 AU (6.8×10^3 yr), 0.6 AU (9.1×10^3 yr), and 0.7 AU (1.6×10^4 yr) are shown. The nearly horizontal lines are $\Sigma_{\rm dust0}$ and $10\Sigma_{\rm dust0}$. The vertical dotted line is the initial snow line.

The mass of the ejected silicate cores is a fraction f of the mass loss of the aggregate in Figure 2. Figure 3 shows the dust surface density distribution as a function of r. The initial radii R_0 of the aggregates are 5, 10, 15, 20, 40, 80, and 100 cm. Each distribution has a peak with an exponential slope on the right-hand side and a sharp decline on the left-hand side. For $R_0 =$ 10 cm, the peak is located at around 3.6 AU, which corresponds to the location where the aggregate radius decreases sharply (see Figure 2).

Figure 3 shows the final dust surface density distribution when all the icy dust aggregates initially located between 5 and 45 AU have fallen and sublimated. All the peaks of the dust surface density exceed the curve labeled by $10\Sigma_{\rm dust0}$, which is an approximate criterion of the gravitational instability.

On the right-hand side of the peak, the sublimation rate is low because the temperature is low in the outer region. In this region, the infall velocity is nearly constant because the radius of an aggregate does not change. Then, the dust surface density (Equation (11)) is proportional to the equilibrium vapor pressure of H_2O (from $dM_i/dr = (dM_i/dt)/(dr/dt) \propto N/(dr/dt)$ in Equation (11), and from N being proportional to the equilibrium vapor pressure) on the right-hand side of the peak, provided that the infall velocity is constant.

As infall proceeds, the temperature increases further. The radius of the icy dust aggregate suddenly decreases, because the sublimation rate exponentially depends on temperature T. On the other hand, the infall velocity decreases with R. The dust surface density $\Sigma_{\rm dust}$ then reaches a peak and sharply drops to zero.

The position of the peak is determined by $\tau_{\rm sub} = \tau_{\rm infall}$, where the sublimation timescale $\tau_{\rm sub} = R_0/(dR/dt)$ is obtained from Equation (7). The infall timescale $\tau_{\rm infall}$ is given by $L/(dr/dt)$, where $L = 0.05$ AU is independent of R_0 from our numerical simulation. The peak position depends on the initial radius R_0 of an icy dust aggregate, as shown in Figure 3. The peak position shifts inward as R_0 because the infall velocity increases with R_0.

There should be a size distribution of the aggregate. The dust surface density distribution is therefore a superposition of the distributions shown in Figure 3 with the weight proportional to the size distribution. The width of the peak in the dust surface distribution is as wide as ~ 1 AU in this case. The concentration of the dust by sublimation is not effective for $P_{\rm H_2O} = 0$ case.

Note that the peaks of the dust surface density for $R_0 \leqslant 40$ cm are beyond the snow line. If $P_{\rm H_2O} \neq 0$ in Equation (7), the sublimation of an icy dust aggregate does not proceed beyond the snow line. In this case, the aggregates with initial radii of $R_0 \leqslant 40$ cm sublimate immediately after passing through the snow line.

5.2. $P_{\rm H_2O} \neq 0$

The icy dust aggregates sublimate only within the snow line in this case. Figure 4 shows the time evolution of the dust surface density when $P_{\rm H_2O} \neq 0$. The initial radius of the aggregate is $R_0 = 10$ cm. The dust surface density increases exponentially inward and decreases sharply at the shifted snow line.

The aggregate with a 10 cm radius sublimates at around 3.6 AU if we neglect the H_2O vapor pressure as shown in the previous subsection. Because the initial position of the snow line (3.0 AU) is within 3.6 AU, the temperature of the snow line is higher than that at 3.6 AU. The timescale of sublimation at the shifted snow line is very short (= 9.3 yr at 3.0 AU). Therefore, an aggregate sublimates instantly when it passes the snow line, and the H_2O vapor sublimating from an icy dust aggregate accumulates within the snow line. The infall of the aggregate occurs only 5×10^{-3} AU from the snow line during sublimation.

The H_2O vapor pressure eventually becomes equal to the equilibrium vapor pressure within the snow line. In this condition, an icy dust aggregate cannot sublimate in the saturated region. As a result, the distribution of the dust surface density is proportional to the equilibrium H_2O vapor pressure. The dust surface density evolves from right to left in Figure 4. $\delta(t)$ is the distance between the initial snow line and the snow line at time t. $\delta = 0.1$, 0.2, 0.3, 0.4, 0.5, 0.6, and 0.7 AU correspond to $t = 6.3 \times 10^2$, 1.6×10^3, 3.0×10^3, 4.8×10^3, 6.8×10^3, 9.1×10^3, and 1.6×10^4 yr, respectively. The peak of the dust surface density distribution reaches $10\Sigma_{\rm dust0}$ when $\delta = 0.4$ AU ($t = 4.8 \times 10^3$ yr).

From right to left, the distributions shown in Figure 4 are formed by the sublimation of icy dust aggregates initially placed

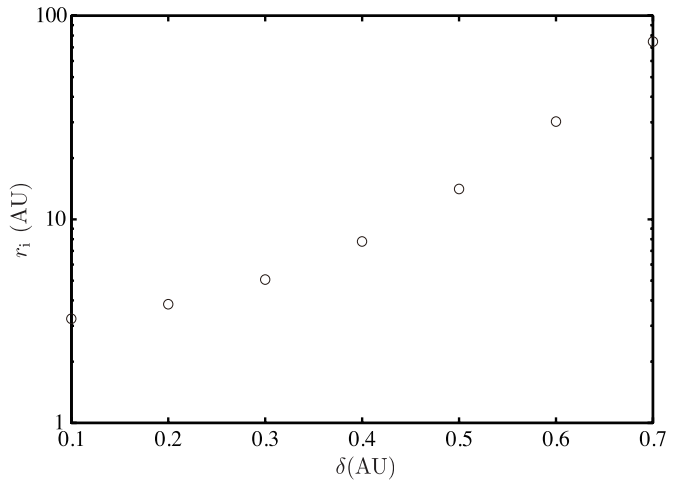

Figure 5. Relationship between the width δ of the region where silicate cores are suspended and the initial position r_i of the outermost aggregate that produces the suspended region.

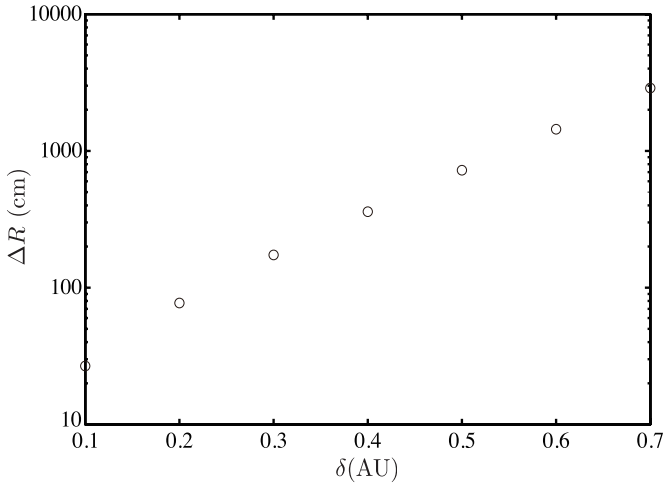

Figure 6. Relationship between δ and ΔR.

between the initial snow line (3.0 AU) and r_i =3.8, 5.1, 7.8, 14.1, 30.2, and 74.6 AU, respectively. Figure 5 represents the relationship between δ and r_i. r_i increases exponentially with δ. It does so because the equilibrium water vapor pressure increases exponentially with temperature. Figure 4 shows that the peak of the curve reaches the critical dust surface density when there is infall of aggregates between 3.0 and 7.8 AU. The width of the infall area is considerably smaller than that in the previous subsection (5 and 45 AU).

It should be noted that the above results do not depend on the size of the aggregate because the sublimation proceeds instantly after the passage of the snow line. Therefore, Figure 4 remains the same even if there is a distribution in size of the aggregate.

5.3. Sweeping

As described in Section 4.3, we start with the density distribution obtained in the previous subsection. Aggregates having a radius of R_0 sweep the suspended silicate cores under the assumption of perfect sticking. Figure 6 shows the relationship between the increase in the radius ΔR of an infalling aggregate and the width of the silicate suspension region δ. ΔR increases exponentially with δ, from the density distribution obtained in Section 5.2, which is determined from the equilibrium vapor pressure. Note that the radius of the infalling aggregate ($R_0 + \Delta R$) exceeds the radius ($R = 2.2 \times 10^2$ cm) at which the infall velocity is at a maximum between $\delta = 0.3$ and 0.4 AU.

Figure 7 shows the dust surface density distribution as a function of r. Each solid curve corresponds to different δ in which the sweeping proceeds. When $\delta = 0.1$ AU, the peak of the dust surface density reaches $10\Sigma_{\rm dust0}$. Comparing Figures 4 and 7, it can be seen that the sweeping effect substantially enhances the peak of the dust surface density distribution.

The timescale required for sweeping is short: 8.5, 1.7, 0.31, 5.0×10^{-2}, 7.3×10^{-3}, 1.4×10^{-3}, and 1.1×10^{-3} yr from $\delta = 0.1$ to 0.7 AU, respectively.

When δ is small ($\delta = 0.1$ AU), ΔR is small as well. In this case, the timescale for sublimation $\tau_{\rm sub}$ is shorter than that for infall $\tau_{\rm vinfall}$. Therefore, the surface density distribution has a maximum at the snow line and it monotonically decreases with r. As δ increases from 0.1 AU, ΔR increases. This increase in ΔR leads to a decrease in $\tau_{\rm infall}$ because the infall velocity increases

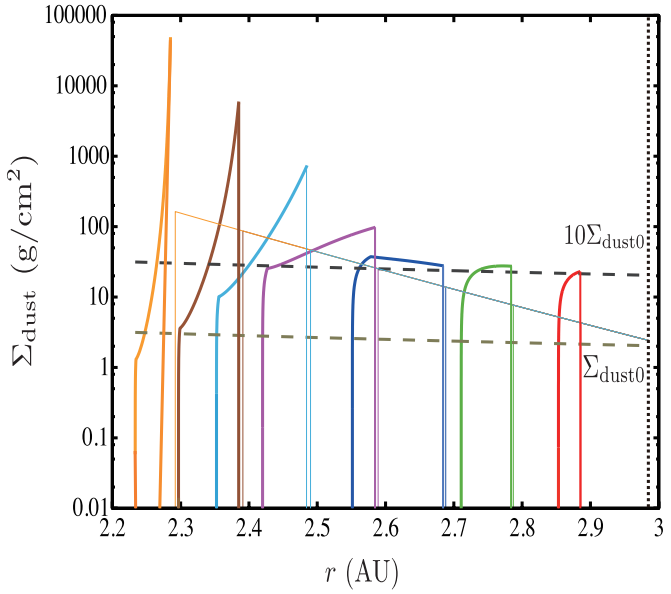

Figure 7. Dust surface density distributions as a function of r, including the sweeping effect. From right to left, the width δ of the region of the silicate core suspension is 0.1, 0.2, 0.3, 0.4, 0.5, 0.6, and 0.7 AU. The nearly horizontal lines are $\Sigma_{\rm dust0}$ and $10\Sigma_{\rm dust0}$: the latter is an approximate criterion for gravitational instability. The thin solid lines are the distributions shown in Figure 4 for comparison. The vertical dotted line is the initial snow line.

(A color version of this figure is available in the online journal.)

as R. Then, the dust surface density distribution becomes flat at the snow line ($\delta = 0.2$ AU in Figure 7) and increases inward ($\delta = 0.3$ AU). In the last case, $\tau_{\rm sub} > \tau_{\rm infall}$ is satisfied at the snow line and a peak appears within the snow line, as shown in Figure 3.

A further increase in δ changes the dust surface density distribution drastically. When R exceeds 2.2×10^2 cm, the infall velocity *increases* as R decreases. This is the case when ΔR is sufficiently large. In this case, the peak of the surface density distribution is observed again at the snow line and the distribution decreases monotonically inward because $\tau_{\rm sub} < \tau_{\rm infall}$ at the snow line. The width of the distribution decreases as δ, because the temperature is high and the sublimation rate is large when r is small (δ is large).

It should be noted that the heights of the peaks are almost the same for $\delta \leqslant 0.3$ AU. The height is proportional to $1/(\tau_{\rm sub} V_r)$.

As δ increases, ΔR and V_r increase. Nevertheless, this increase in V_r is compensated by the decrease in $\tau_{\rm sub}$, caused by the temperature increase.

As δ increases from 0.3 to 0.4 AU, V_r passes its peak and begins to decrease. An aggregate then shrinks at the snow line down to a radius where V_r is at a maximum without substantial infall. The peak of the surface density is observed at the snow line, and the distribution decreases monotonically. The width decreases as δ because the temperature at the snow line increases as the snow line shifts inward.

It should be noted that the results do not depend on the size of the aggregate because the aggregate grows substantially by sweeping (see Figure 6). Even if the size of the aggregate is smaller than the assumed, the size grows by sweeping and the resultant dust surface density does not change. If the size of the aggregate is much larger than the assumed size, $\sim$10 m, the shape of the peak is similar to those shown in the leftmost curve in Figure 7. However, such a large size of the infalling aggregate is unreasonable based on the numerical simulations (Brauer et al. 2008).

The aggregates collide with each other as they infall. Typical collision velocity is $\sim 10\,{\rm m\,s^{-1}}$ for the aggregate sizes shown in Figure 6. The most possible outcomes of a collision are fragmentation because sintering proceeds around the snow line (S.-i. Sirono 2011, in preparation). Because the size of the fragments is much smaller than that of the original size, the infall velocity of the fragments is small. This reduction in infall velocity makes the width of the peak narrow and the height of the peak increase from those shown in Figure 7.

In reality, the ejection of the silicate core and the sweeping proceed simultaneously. If the increase in the size of the aggregate is considerably smaller than those shown in Figure 6, the dust surface density distribution may change from those in Figure 7. When $\sim$10 cm sized aggregates are formed and infall begins, the silicate cores are ejected and sweeping begins. If sweeping does not proceed, $\Delta R = 0$ and the width of the sublimation region is 5×10^{-3} AU as shown in Section 4.2. Suppose the silicate core density immediately within the snow line is $\rho_{\rm d}$ and the snow line moves inward at a velocity of $V_{\rm sn}$. The flux of the silicate core through the snow line is $\rho_{\rm d} V_{\rm sn}$. This flux is swept by the infalling aggregates. If an aggregate grows by ΔR through sweeping, the increase in mass of an aggregate is $S_{\rm d}\rho_{\rm mat}\Delta R$, provided $\Delta R \ll R$, where $S_{\rm d}$ is the cross-section of an aggregate. The flux of the sweeping aggregate per unit time and unit area is written as $n_{\rm d} V_r$, where $n_{\rm d}$ is the number density of the infalling aggregate. Multiplying these expressions gives $n_{\rm d} V_r S_{\rm d} \rho_{\rm mat} \Delta R$ as the sweeping rate per unit time and unit area. It should be noted that this expression is valid for $\Delta R \ll R_0$. Because the timescale for sweeping is short as shown before, a steady state is quickly attained. Equating these two expressions leads to

$$\Delta R = \frac{V_{\rm sn}\rho_{d0}}{\rho_{\rm mat} n_d S_d V_r} \simeq R_0 \frac{\Sigma V_{\rm sn}}{\Sigma_{\rm dust0} V_r}, \qquad (15)$$

where Σ is the dust surface density immediately within the snow line. When the snow line is in its initial position, $V_{\rm sn} = 1.6 \times 10^{-4}\,{\rm AU\,yr^{-1}}$ and $V_r = 5.5 \times 10^{-4}\,{\rm AU\,yr^{-1}}$ for 10 cm sized aggregates give $V_{\rm sn}/V_r = 3.4$. Therefore, $\Delta R \sim R_0$ is attained if $\Sigma/\Sigma_{\rm dust0} \simeq 1$. Although we assume $\Delta R \ll R_0$, ΔR cannot be neglected even before the increase in Σ. The size of the aggregate and the infall velocity should increase from the initial conditions. As a result, the surface density distribution would not be substantially changed, even if we take into account the simultaneity of ejection and sweeping.

6. DISCUSSION

6.1. Effects of Turbulence

The rotational velocity of the region in which silicate cores are suspended is higher than that of the gaseous region, where the force of the gas pressure gradient is effective. The velocity difference between two regions may induce turbulence. Moreover, in the early stage of a protoplanetary nebula, global turbulence may develop, although its formation mechanism remains controversial.

Turbulence induces diffusion of the silicate cores and H_2O vapor both radially and vertically. The diffusion constant of the silicate cores is given by $\alpha h_{\rm gas}^2 \Omega_k$, based on the α turbulence model (Dubrulle et al. 1995).

If the amount of silicate cores' radial diffusion within the snow line is significant, the height of the peaks shown in Figure 7 would decrease. The silicate cores' outward diffusion is negligible because they will be swept by infalling aggregates on a short timescale. It should be noted that the snow line moves *inward* as sublimation proceeds. Suppose the dust density at the peak of the dust surface density distribution is $\rho_{\rm d}$. If the diffusion distance is denoted by L, the rate of the dust density increase within the snow line followed by the movement of the snow line is roughly given by $\rho_{\rm d} V_{\rm sn}/L$. On the other hand, the density decrease rate due to diffusion is given by $\alpha h_{\rm gas}^2 \Omega_{\rm k} \rho_{\rm d}/L^2$. Equating these two expressions gives us $L = \alpha h_{\rm gas}^2 \Omega_k / V_{\rm sn} = 2.4\alpha$ AU. Because $\alpha \ll 1$ in many cases, the inward diffusion of silicate cores within the snow line is also negligible as compared to the width $\simeq$0.1 AU of the surface density distributions shown in Figure 7.

The inward diffusion of H_2O vapor can be treated by the same argument presented above, because the molecular diffusion of H_2O vapor can be neglected compared to the turbulence diffusion. The H_2O vapor and the silicate core diffuse in the same way. The diffusion length scale due to turbulence is 2.4α AU, much smaller than the width of the resultant surface density distribution. Therefore, the inward diffusion of H_2O vapor can be neglected.

Next, we discuss the outward diffusion of H_2O. Like silicate cores, the H_2O saturated gas in the sublimation region diffuses outward. The H_2O vapor condenses onto the silicate cores because the temperature decreases. The icy dust aggregates from outside, as described in the previous section, and sweep the silicate cores that are covered by re-condensed icy mantle. Therefore, we cannot expect the accumulation of icy particles just outside of the snow line as predicted by Stepinski & Valageas (1997), Cuzzi & Zahnle (2004) and Ciesla & Cuzzi (2006).

Stevenson & Lunine (1988) discussed a similar problem. They considered the outward diffusion of H_2O vapor initially located inside the snow line with the solar abundance. In their work, the H_2O vapor condenses just outside the snow line and the solid ice accumulates there. Although neglected, the snow line should shift inward as the outward diffusion of the H_2O vapor because the region inside the snow line is saturated by the diffused H_2O vapor. This effect reduces the width of the peak of the dust surface density distribution shown in Figure 7 because the sublimation rate of the infalling aggregate increases as temperature followed by the inward shift of the snow line.

The sweeping aggregate sublimates the H_2O ice again around the snow line. Note that the curves shown in Figure 7 are based on the assumption that the sublimation of H_2O ice and the ejection of silicate cores proceed from the surface of the

aggregate. However, the ejection of silicate cores might be much faster than that shown in Figure 7, because the temperature distribution within the aggregate is homogeneous, provided that the timescale of thermal diffusion is short compared to the timescale of infall of an aggregate. The sublimation of H_2O proceeds at the same rate in the entire aggregate in this case. The connection between grains by the recovered H_2O ice is cut simultaneously, both deep within the aggregate and on the surface of the aggregate. If this is the case, the peaks shown in Figure 7 should be higher.

If the silicate cores diffuse vertically, the sweeping rate of the infalling aggregate decreases. Because the sweeping proceeds only beyond the snow line, the cores have time to diffuse until they are involved by the snow line. The cores ejected close to the snow line do not have enough time to diffuse because the snow line passes the region in a short timescale. On the other hand, the cores ejected at the region far from the snow line can diffuse vertically. The time available for diffusion is $\sim 10^3$ yr, because the width of the peak is $\sim$0.1 AU and the velocity of the snow line is $\sim 10^{-4}$ AU yr^{-1}. When the snow line involves the region, the infalling aggregate starts to sweep them. The timescale for sweeping is simply the same as the diffusion time of $\sim 10^3$ yr. Taking account of the fact that the cores suspended in the region close to the snow line are efficiently swept, the fraction of the cores avoiding the sweeping is less than half of the ejected cores. Therefore, ΔR slightly decreases, and the widths of the peaks shown in Figure 7 decrease because the infalling velocity decreases. It should be noted that the heights of the peaks are almost the same if $\delta \leqslant 0.3$ AU. The decrease in ΔR only results in the decrease in the width of the peaks. The heights of the peaks remain the same even if the vertical diffusion proceeds for $\delta \leqslant 0.3$ AU. On the other hand, the heights of the peaks for $\delta \geqslant 0.4$ AU will decrease because the heights are proportional to the amount of the swept cores.

6.2. Possibility of Observation

The contrast between the dust surface density at the peak and in the surrounding region is more than a factor of 10. Paardekooper & Mellema (2004) showed that an enhancement in the dust surface density distribution with a contrast of a factor of 3 produced by a planet at 5.2 AU is detectable by ALMA (Atacama Large Millimeter/submillimeter Array). They adopted a Gaussian smoothing length of 2.5 AU (corresponding to a distance to an object of 140 pc) to simulate the maximum resolution of ALMA. On the other hand, the enhancement of the dust surface density is more than 10 in this study. Therefore, an increase in the thermal emission from dust might be observed by ALMA.

Recent observations by the *Spitzer Space Telescope* revealed the common existence of H_2O vapor in a protoplanetary nebula. Most of the vapor is considered to be formed in the warm region of the nebula by gas phase chemical reactions (Bethell & Bergin 2009). However, the dynamical migration due to infalling might play a role (Glassgold et al. 2009). Observational results are well explained by a radiative transfer model under the assumption that the H_2O abundance drops off by many orders of magnitude at around 1 AU (Meijerink et al. 2009). The depletion is caused by the condensation of H_2O vapor as they move vertically to the cold region below the warm surface region. Based on this, the location of the snow line at the midplane can be constrained by radial distribution of water vapor. The inward drift of the snow line predicted by this paper might be confirmed as the correlation between the disk age and the position of the snow line.

6.3. Planets Formed from a Planetesimal Ring

According to the results of this study, rocky planetesimals are formed in a particular region in a protoplanetary nebula. The location of this region is determined by the snow line of H_2O ice. Morishima et al. (2008) performed an *N*-body numerical simulation for the period from the initial swarm of planetesimals to the formation of planets. The initial condition of their simulation is a compact planetesimal belt with a width of 0.3–0.5 AU, a value that was essentially chosen because of limitations in the computational cost. Interestingly, this compact planetesimal belt consistently reproduces the arrangement of solar system planets. Their simulation results suggest that the limited distribution of planetesimals obtained in this study is consistent with the formation of solar system planets.

7. CONCLUSION

In this study, we have demonstrated that the ejection of silicate cores from icy aggregates caused by the sublimation of H_2O ice is an effective mechanism for an enhancement of dust surface density distribution that is sufficient to trigger the gravitational instability that could form planetesimals. We have studied three cases: with and without H_2O vapor in the gaseous nebula, and with H_2O vapor, including the sweeping effect of infall icy dust aggregates. The dust surface density is increased by more than a factor of 10 in reasonable timescales. The sweeping is especially effective and the timescale for this enhancement is less than $\sim$ 600 yr after the formation of 10 cm sized aggregates. In this study, the location of the snow line is 3 AU based on the temperature distribution of Hayashi model. The temperature distribution and the location of the snow line depend on the luminosity of the central star. However, the mechanism proposed here is effective independent of the activity of the central star.

We have discussed the effect of turbulence, whose origin may be in the velocity difference between the dust and the gas regions. Such turbulence could promote the increase in the dust surface density, because the re-condensation of H_2O vapor leads to the formation of an H_2O ice layer on the ejected silicate cores (or aggregates) that are swept by infalling aggregate. This layer sublimates within the snow line and promotes the disconnection of the swept silicate cores.

The authors deeply appreciate the critical comments by an anonymous referee. The authors are grateful to Dr. N. Ishitsu, S. Watanabe, and M. Arakawa for helpful discussions. This work was supported by the Global COE Program of Nagoya University "Quest for Fundamental Principles in the Universe (QFPU)" from JSPS and MEXT of Japan.

REFERENCES

Bethell, T., & Bergin, E. 2009, Science, 326, 1675
Brauer, F., Dullemond, C. P., & Henning, Th. 2008, A&A, 480, 859
Chavanis, P. H. 2000, A&A, 356, 1089
Ciesla, F. J., & Cuzzi, J. N. 2006, Icarus, 181, 178
Cuzzi, J. N., Hogan, R. C., Paque, J. M., & Dobrovoslskis, A. R. 2001, ApJ, 546, 496
Cuzzi, J. N., & Zahnle, K. J. 2004, ApJ, 614, 490
Dubrulle, B., Morfill, G., & Sterzik, M. 1995, Icarus, 114, 237
Glassgold, A. E., Meijerink, R., & Najita, J. R. 2009, ApJ, 701, 142
Goldreich, P., & Ward, W. R. 1973, ApJ, 183, 1051
Greenberg, J. M. 1998, A&A, 330, 375

Hayashi, C., Nakazawa, K., & Nakagawa, Y. 1985, in Protostars and Planets II, ed. D. C. Black & M. S. Matthews (Tucson, AZ: Univ. Arizona Press), 1100
Johansen, A., Oishi, J. S., Mac Low, M.-M., Klahr, H., Henning, Th., & Youdin, A. 2007, Nature, 448, 1022
Meijerink, R., Pontoppidan, K. M., Blake, G. A., Poelman, D. R., & Dullemonde, C. P. 2009, ApJ, 704, 1471
Morishima, R., Schmidt, M. W., Stadel, J., & Moore, B. 2008, ApJ, 685, 1247
Nakagawa, Y., Sekiya, M., & Hayashi, C. 1986, Icarus, 46, 375
Paardekooper, S.-J., & Mellema, G. 2004, A&A, 425, L9
Sekiya, M. 1998, Icarus, 133, 298
Stepinski, T. F., & Valageas, P. 1997, A&A, 319, 1007
Stevenson, D. J., & Lunine, J. I. 1998, Icarus, 75, 146
Throop, H. B., & Bally, J. 2005, A&A, 623, L149
Wada, K., Tanaka, H., Suyama, T., Kimura, H., & Yamamoto, T. 2009, ApJ, 702, 1490
Weidenschilling, S. J. 1977, MNRAS, 180, 57
Yamamoto, T., Nakagawa, N., & Fukui, Y. 1983, A&A, 122, 171
Youdin, A. M., & Shu, F. H. 2002, ApJ, 580, 494